TYPE Original Research
PUBLISHED 09 January 2024
DOI 10.3389/fspas.2023.1284913

Check for updates

OPEN ACCESS

EDITED BY
Robert James Leamon,
University of Maryland, United States

REVIEWED BY
Zdenek Nemecek,
Charles University, Czechia
Nils Janitzek,
ETH Zürich, Switzerland

*CORRESPONDENCE
E. Johnson,
ejohn@udel.edu

RECEIVED 29 August 2023
ACCEPTED 13 December 2023
PUBLISHED 09 January 2024

CITATION
Johnson E, Maruca BA, McManus M, Stevens M, Klein KG and Mostafavi P (2024), Application of collisional analysis to the differential velocity of solar wind ions.
Front. Astron. Space Sci. 10:1284913.
doi: 10.3389/fspas.2023.1284913

Application of collisional analysis to the differential velocity of solar wind ions

E. Johnson[1]*, B. A. Maruca[1], M. McManus[2], M. Stevens[3], K. G. Klein[4] and P. Mostafavi[5]

[1]Department of Physics and Astronomy, University of Delaware, Newark, DE, United States, [2]Department of Physics, University of California, Berkeley, CA, United States, [3]Center for Astrophysics, Harvard University, Cambridge, MA, United States, [4]Lunar and Planetary Laboratory, University of Arizona, Tucson, AZ, United States, [5]The Johns Hopkins University Applied Physics Laboratory, Laurel, MD, United States

Collisional analysis combines the effects of collisional relaxation and large-scale expansion to quantify how solar wind parameters evolve as the plasma expands through the heliosphere. Though previous studies have applied collisional analysis to the temperature ratio between protons (ionized hydrogen) and α-particles (fully ionized helium), this is the first study to explore α-proton differential flow with collisional analysis. First, the mathematical model for the collisional analysis of differential flow was derived. Then, this model was applied to individual *in-situ* observations from Parker Solar Probe (PSP; $r = 0.1$–0.27 au) to generate predictions of the α-proton differential flow in the near-Earth solar wind. A comparison of these predicted values with contemporaneous measurements from the Wind spacecraft ($r = 1.0$ au) shows strong agreement, which may imply that the effects of expansion and Coulomb collisions have a large role in governing the evolution of differential flow through the inner heliosphere.

KEYWORDS

solar wind, plasma, collision physics, Coulomb collisions, differential flow, Sun, heliosphere

1 Introduction

The solar wind ions consist of protons (ionized hydrogen), a small but variable percentage (typically ≈4% and ≲ 20%; Kasper et al., 2012) of α-particles (fully ionized helium), with trace amounts of heavier ions (Schmelz et al., 2012). Solar wind plasma often shows deviations from local thermal equilibrium (LTE) (Griem, 1963), in which, for example, the ion species exhibit distinct temperatures and bulk speeds (Marsch, 2006; Verscharen et al., 2019). Once generated, these non-LTE features are preserved by the solar wind's high temperature and low density, which reduces the rate of Coulomb collisions—"soft," small-angle deflections between charged particles mediated by the electrostatic force. These collisions, which allow the particles to exchange energy and momentum in "collisional relaxation," serve as the ultimate drivers of thermal equilibrium (Hernández and Marsch, 1985; Livi et al., 1986). The time required for collisions to substantially reduce a given non-LTE feature is the "collisional timescale," with the process being unique for each parameter and system configuration (e.g., the "slowing-down time" for the difference in bulk speed).

For example, considerable attention has been given to the difference in proton and α-particle temperatures, which can be quantified by the ratio

$$\theta_{\alpha p} = \frac{T_\alpha}{T_p}, \tag{1}$$

where T_α is the scalar temperature of the α-particles and T_p is the proton scalar temperature. Early studies (Feldman et al., 1974; Neugebauer, 1976; Marsch et al., 1982) found that typically $\theta_{\alpha p} \gtrsim 1$ and that $\theta_{\alpha p}$ is strongly anti-correlated with "Coulomb number," the ratio of the expansion time to the collisional timescale. This finding, which was later confirmed by Kasper et al. (2008), Maruca et al. (2013), and Tracy et al. (2015), was interpreted as indicating that α-particles are preferentially heated relative to the protons in the solar corona and that Coulomb collisions slowly thermalize these two species as the plasma expands.

Though Coulomb number is a useful tool in understanding collisional thermalization, Maruca et al. (2013) introduced "collisional analysis" to provide a more quantitative method for studying $\theta_{\alpha p}$ (Eq. 1). In this technique, basic models for the solar wind's expansion are incorporated into the equations of collisional relaxation, this generates a prediction for how $\theta_{\alpha p}$ in a given parcel of plasma varies with distance, r, from the Sun. Maruca et al. (2013) applied this technique to individual $\theta_{\alpha p}$-measurements from the Wind spacecraft ($r = 1.0$ au) to predict the distribution of $\theta_{\alpha p}$-values at $r = 0.1$ au, i.e., near-Sun solar wind. This prediction was confirmed by Johnson et al. (2023), who further validated the collisional analysis technique by showing that it could be applied to $\theta_{\alpha p}$-measurements from Parker Solar Probe (PSP; $r = 0.1$–0.27 au) to effectively predict contemporaneous measurements of $\theta_{\alpha p}$ from Wind.

This study extends collisional analysis to model the collisional effects on "differential flow," which is the difference in the bulk velocities of two ion species:

$$\Delta \mathbf{v}_{ij} = \mathbf{v}_i - \mathbf{v}_j, \tag{2}$$

where $\mathbf{v}_i$ and $\mathbf{v}_j$ are the bulk velocities of i- and j-particle species, respectively. Just as α-particles are observed to typically be hotter than protons ($T_\alpha > T_p$), they are also typically faster than the protons ($|\mathbf{v}_\alpha| > |\mathbf{v}_p|$). Likewise, prior studies have shown that $|\Delta \mathbf{v}_{\alpha p}|$ anti-correlates with Coulomb number just as $\theta_{\alpha p}$ does (Kasper et al., 2008; Alterman et al., 2018). Nevertheless, the extended collisional analysis technique described herein offers a more quantitative examination of collisional slowing of ion species in the solar wind.

Section 2 derives the mathematical model for the collisional analysis of differential flow. In Section 3, this model is applied to measurements from PSP to generate predictions of the near-Earth solar wind that are then compared to contemporaneous Wind observations. Concluding remarks are presented in Section 4.

2 Background

Coulomb number (N_C) was used in earlier studies, such as Neugebauer (1976), Marsch et al. (1982) and Neugebauer and Feldman (1979), to demonstrate that $|\Delta \mathbf{v}_{\alpha p}| \to 0$ and $\theta_{\alpha p} \to 1$ as N_C increases Verscharen et al. (2019, Fig 13). However, N_C assumes that plasma parameters remain constant and do not scale with distance, yet plasma parameters, such as those of temperature and density, have strong radial trends. To address these issues works by Hernández et al. (1987), Kasper et al. (2017) and Kasper and Klein (2019) use an integral form of the Coulomb number known as the collisional age, which accounts for radial dependencies of plasma parameters. Collisional analysis was introduced by Maruca et al. (2013), combining the effects of expansion and Coulomb collisions on ion temperature ratios in any given parcel of solar wind plasma. A full in-depth review on collisional analysis is presented in Maruca et al. (2013), with Johnson et al. (2023) applying this technique to PSP data for the first time. This section presents a variation of collisional analysis that, for the first time, addresses ion differential flow rather than differences in ion temperature.

The rate at which the differential flow, $\Delta \mathbf{v}_{ij}$ (Eq. 2), between i- and j-particles is eroded by Coulomb collisions is given by (Richardson, 2019):

$$\frac{d\Delta \mathbf{v}_{ij}}{dt} = -\nu_{ij}^{(s)} \Delta \mathbf{v}_{ij}, \tag{3}$$

where t is time, and $\nu_{ij}^{(s)}$ is the collision frequency for the reduction of differential flow between i- and j-particles. Richardson (2019); Larroche (2021) expresses this as:

$$\nu_{ij}^{(s)} = \left(1 + \frac{m_i}{m_j}\right) \psi\left(\frac{m_j v_i^2}{2 k_B T_j}\right)\left(\frac{4\pi q_i^2 q_j^2 n_j}{m_i^2 v_i^3}\right)\lambda_{ij}, \tag{4}$$

where, for i-particles, m_i is mass, q_i is charge, v_i is the bulk velocity, T_i is scalar temperature, n_i is number density and k_B is the Boltzmann constant. The Coulomb logarithm, λ_{ij}, for the collision of an i- and j-particle (i.e., mixed ion-ion collisions) is (Richardson, 2019):

$$\lambda_{ij} = 23 - \ln\left[\frac{Z_i Z_j (\mu_i + \mu_j)}{\mu_i T_j + \mu_j T_i}\left(\frac{n_i Z_i^2}{T_i} + \frac{n_j Z_j^2}{T_j}\right)^{1/2}\right], \tag{5}$$

with $\mu_i = m_i / m_p$, $Z_i = q_i / q_p$, where m_p and q_p are the proton mass and charge. The ψ function for any given x-value is defined to be

$$\psi(x) = \frac{2}{\sqrt{\pi}} \int_0^x e^{-t} \sqrt{t}\, dt = 1 - \frac{2\Gamma(3/2, x)}{\sqrt{\pi}}, \tag{6}$$

where Γ denotes the incomplete gamma function (Arfken and Weber, 2011). The derivation directly models the collisional thermalization of two ion species. This is achieved by considering a multi-species plasma with no relative drift or temperature anisotropy (Maruca et al., 2013; Richardson, 2019).

Following the example in Maruca et al. (2013), the collision rate can be converted from a time derivative to one with respect to distance, r. The system is assumed to be in steady state, other deviations from equilibrium are neglected and $\eta_{ij} = n_i / n_j$ remains constant in any parcel of plasma. Under the assumption that the plasma is radially streaming from the Sun in steady state,

$$\frac{d\Delta \mathbf{v}_{ij}}{dr} = \frac{d\Delta \mathbf{v}_{ij}}{dt}\frac{dt}{dr} = \frac{1}{v_p}\frac{d\Delta \mathbf{v}_{ij}}{dt}, \tag{7}$$

where the solar wind speed is approximated as the proton bulk speed, $v_p = |\mathbf{v}_p|$, i.e., the background particle speed.

In line with Maruca et al. (2013) and for the specific case of α-particles drifting relative to protons, only protons and α-particles

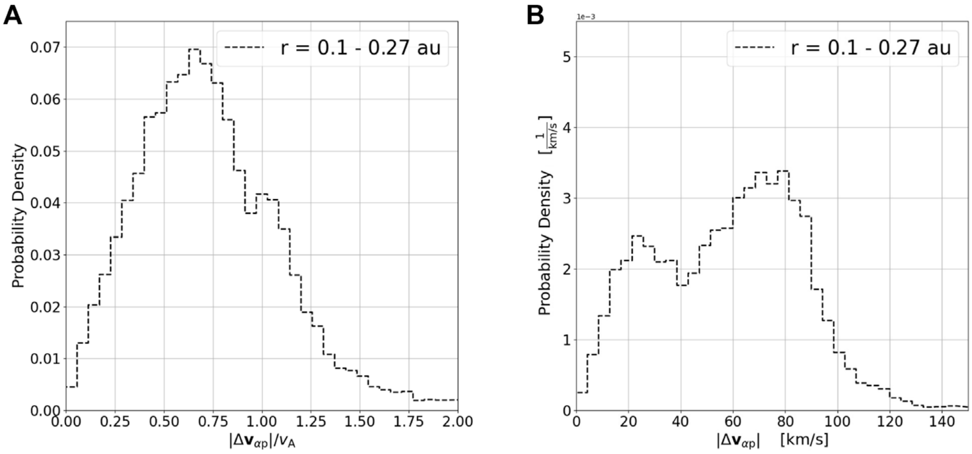

FIGURE 1
Histogram of observed values of α-proton differential flow: **(A)** normalized $|\Delta \mathbf{v}_{\alpha p}|/v_A$ and **(B)** unnormalized $|\Delta \mathbf{v}_{\alpha p}|$ from the PSP data set (r =0.1 to 0.27 au). Bin counts have been normalized to approximate probability density.

were considered: other ion species and electrons were neglected. Equations 3–7 combine to give

$$\frac{d\Delta \mathbf{v}_{\alpha p}}{dr} = -\nu_{\alpha p}^{(s)} \frac{\Delta \mathbf{v}_{\alpha p}}{v_p}, \tag{8}$$

with the collision rate,

$$\nu_{\alpha p}^{(s)} = \left(1 + \frac{m_\alpha}{m_p}\right)\left(1 - \frac{2\Gamma\left(\frac{3}{2}, \frac{m_p v_\alpha^2}{2k_B T_p}\right)}{\sqrt{\pi}}\right)\left(\frac{4\pi q_\alpha^2 q_p^2 n_p}{m_\alpha^2 v_\alpha^3}\right)\lambda_{\alpha p}, \tag{9}$$

remaining consistent with prior derivations, such as Hernández and Marsch (1985), Eq. 23 and Spitzer (1962).

On its own, Eq. 8 only models the effects of collisions on $\Delta\mathbf{v}_{\alpha p}$. Nevertheless, the average effects of expansion can be incorporated by allowing density, bulk speed, and scalar temperature to scale with r. For example, Hellinger et al. (2011) utilized Helios observations to conclude that:

$$\begin{aligned} n_p(r) \propto r^{-1.8}, \quad & v_{r,p}(r) \propto r^{-0.2}, \\ T_p(r) \propto r^{-0.74}, \quad \text{and} \quad & B(r) \propto r^{-1.6}. \end{aligned} \tag{10}$$

Scaling in magnetic-field strength, B, is not explicitly required for Eq. 8, and it is not used in any of the collisional analysis. It is only required to normalize $\Delta\mathbf{v}_{\alpha p}$ to the Alfvén speed,

$$v_A = \frac{B}{\sqrt{\mu_0\left(n_\alpha m_\alpha + n_p m_p\right)}}, \tag{11}$$

where μ_0 is the vacuum permeability. These scaling values are used to remain consistent with prior works, such as Maruca et al. (2013) and Johnson et al. (2023). Additionally, the values are not fixed and can be taken from observations or simulations. For example, both Durovcova et al. (2019) and Maruca et al. (2023) provide alternative scaling values, that when implemented produce comparable results when compared to Hellinger et al. (2011).

3 Analysis

The data set used in this study is the same as the one used by Johnson et al. (2023), who provide a detailed discussion of its properties and of the algorithm applied to correct for variations in sampling cadence. The data were derived from ion measurements from the electrostatic analyzer (ESA; Livi et al., 2021) in the SWEAP instrument suite (Kasper et al., 2016) onboard the PSP spacecraft (Fox et al., 2016). Proton and α-particle parameter values were extracted from PSP/SWEAP ESA distribution via a non-linear fitting algorithm. Three distinct ion populations were considered: a proton core, and proton beam, and a single alpha-particle population. Each population was modeled with a bi-Maxwellian VDF. Though the VDF's were allowed to drift relative to one another, proton beam-core drift was only permitted along the magnetic-field axis (McManus et al., 2022; Mostafavi et al., 2022), the α-particle velocities are not constrained in this way. The final data set consisted of 23,770 total data entries spanning approximately three, 10-day intervals[1]; corresponding to three distinct 10-day observation periods from PSP, occurring at three distinct time periods. During those intervals, PSP ranged from $r \approx 0.1$ to 0.27 au.

Figure 1 shows the probability distribution of the α-proton differential flow ($|\Delta\mathbf{v}_{\alpha p}|$, Eq. 2) for the data set, it also shows this distribution normalized by the Alfvén speed ($|\Delta\mathbf{v}_{\alpha p}|/v_A$). The data were sorted among 40 bins spanning $\Delta\mathbf{v}_{\alpha p} = 0$–$200$ km/s and $\Delta\mathbf{v}_{\alpha p}/v_A = 0$ to 2.0. The count of data in each bin was divided by the total number of data and the width of the bin to approximate probability density (Maruca et al., 2011). Poisson statistics determined the average uncertainty to be $\sigma_{\Delta\mathbf{v}_{\alpha p}} = 7.20\,\%$.

1 The first three 10-day encounter was comparably slower (v_p) and denser (n_p) than the later two encounters. Encounters are combined to generate a larger data-set that is more statistically significant and is more representative of an average solar wind stream.

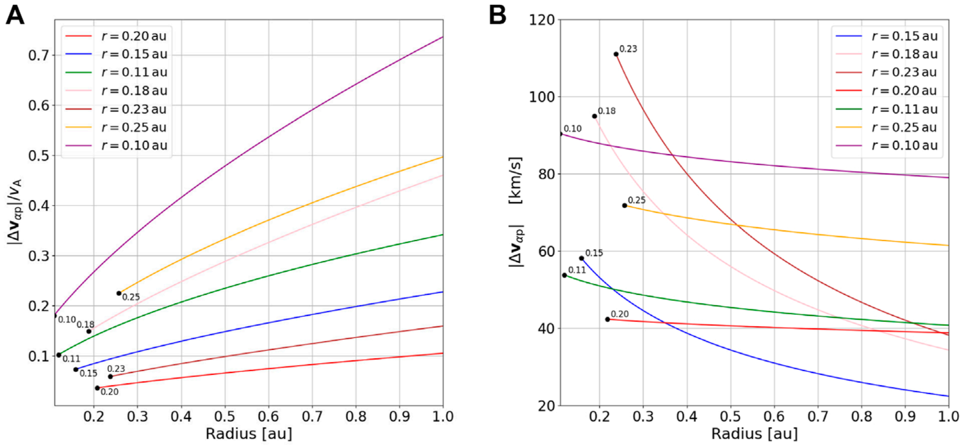

FIGURE 2
Radial evolution of α-proton differential flow: **(A)** normalized $|\Delta \mathbf{v}_{\alpha p}|/v_A$ and **(B)** unnormalized $|\Delta \mathbf{v}_{\alpha p}|$. The black dots are observations from PSP, the colors are a prediction of the differential flow based on that observation. Table 1 provides a detailed overview of these parameters.

TABLE 1 Differential flow values and additional plasma parameters from Figure 2. Start values are from PSP observations, end values are at r =1.0 au and are calculated from collisional analysis.

	$\lvert\Delta \mathbf{v}_{\alpha p}\rvert$ [km/s]		$\lvert\Delta \mathbf{v}_{\alpha p}\rvert/v_A$		n_p [cm^{-3}]		$\eta_{\alpha p}$	v_p [km/s]		T_p [10^6K]		T_α [10^6K]	
r = [au]	Start	End	Start	End	Start	End	-	Start	End	Start	End	Start	End
0.10	90.45	78.99	0.181	0.736	20.49	0.32	0.002	357.3	225.4	1.29	0.21	5.21	0.52
0.11	53.81	40.74	0.102	0.342	8.03	0.15	0.019	407.4	262.0	3.01	0.55	6.80	0.74
0.15	58.14	22.38	0.073	0.228	13.67	0.45	0.013	451.1	308.7	2.24	0.52	4.66	0.70
0.18	94.95	34.36	0.149	0.460	18.49	0.84	0.007	360.8	256.1	2.90	0.77	9.16	1.65
0.20	42.30	38.78	0.036	0.105	14.00	0.77	0.013	466.1	337.8	2.25	0.65	9.31	1.86
0.23	111.01	38.18	0.059	0.159	26.86	1.91	0.008	420.5	313.4	2.43	0.78	8.96	2.06
0.25	71.81	61.44	0.225	0.496	11.88	0.98	0.014	468.7	355.2	2.26	0.78	6.76	1.69

Collisional analysis was applied to the PSP data (r = 0.1–0.27 au) set to predict the values of $|\Delta \mathbf{v}_{\alpha p}|$ in the near-Earth solar wind (r = 1.0 au). A PSP "datum" from this data set consisted of a set of values for n_α, n_p, T_α, T_p, $\mathbf{v}_\alpha$, $\mathbf{v}_p$ and B derived from measurements made a given distance r_0 from the Sun. These are applied as a boundary condition to Eq. 8 and the scaling functions in Eq. 10 are implemented to solve for $\Delta \mathbf{v}_{\alpha p}(r)$.

Figure 2 shows this collisional analysis applied to seven exemplar data from the PSP data set. Black dots indicate the measured values of differential flow and PSP's distance from the Sun at the time. The colored curves show the predicted differential flow values farther from the Sun based on the effects of collisions and expansion. The scaling functions come into play not only in Eq. 8 but also in computing the Alfvén speed (v_A; Eq. 11) for the normalized differential flow ($|\Delta \mathbf{v}_{\alpha p}|/v_A$). Since v_A almost invariably rapidly decreases with distance from the Sun, all of the curves in Figure 2A monotonically increase. In contrast, Figure 2B shows monotonically decreasing curves, which reveal the gradual erosion of differential flow by Coulomb collisions. Some of the curves in Figure 2B cross due to the wide variation in collision rates (Eq. 9) across the PSP data set.

This collisional analysis procedure was applied to all data in the PSP data set to generate a prediction of α-proton differential flow for the near-Earth solar wind (r = 1.0 au). Figure 3 shows the observed differential flow in the near-Sun solar wind compared to the predicted near-Earth differential flow from collisional analysis for an exemplar time interval. It can be seen the α-proton differential flow decreases with distance from the corona.

Figure 4 shows in blue-solid the distribution of these predicted values: (a) normalized to the Alfvén speed and (b) unnormalized. To validate the predicted values, Figure 4 also shows in red-dashed the distribution of α-proton differential flow values measured contemporaneously with the Wind spacecraft (Acuna et al., 1995;

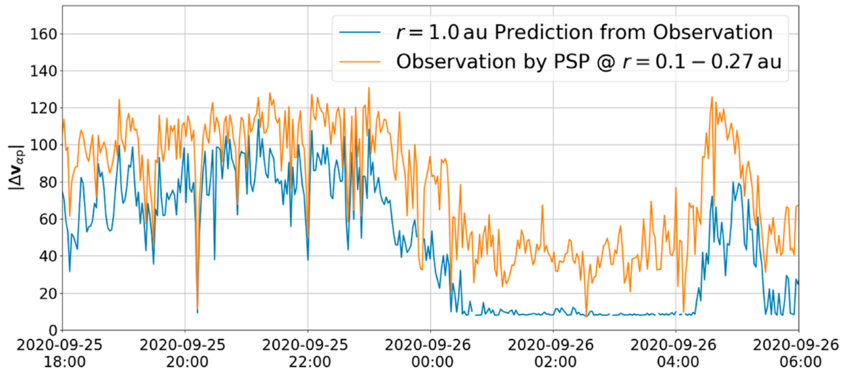

FIGURE 3
Observation from PSP of the α-proton differential flow, prediction from collisional analysis of the near-Earth α-proton differential flow using the observation from PSP.

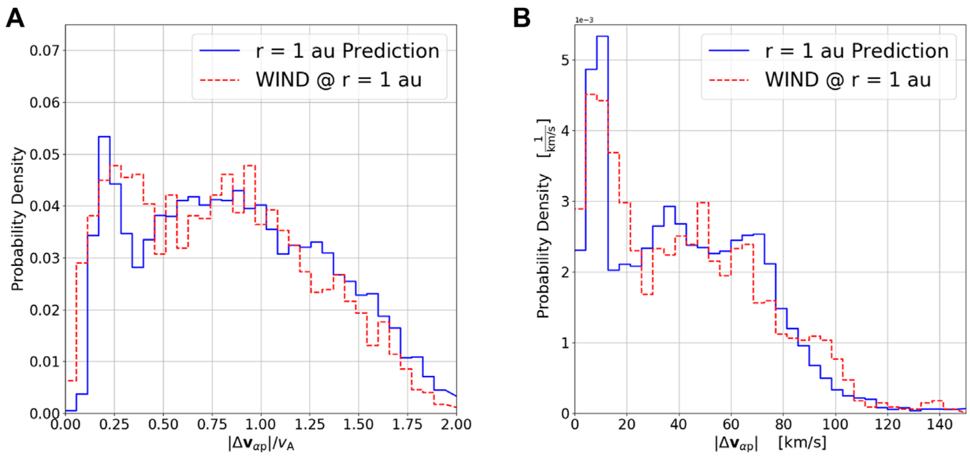

FIGURE 4
Histogram of observed values of α-proton differential flow: **(A)** normalized $|\Delta \mathbf{v}_{\alpha p}|/v_A$ and **(B)** unnormalized $|\Delta \mathbf{v}_{\alpha p}|$ from the Wind data set at r =1.0 au (red dashed). Histogram of predicted α-proton differential flow values at r =1.0 au from the PSP data set based on collisional analysis (blue solid).

Wilson et al., 2021), which orbits in the first Lagrange point (L1) of the Earth-Sun system ($r \approx 1.0$ au from the Sun). The Wind ion measurements shown in Figure 4 are specifically from the Faraday cups in the Solar Wind Experiment (SWE; Ogilvie et al., 1995) and were the same data set as used by Johnson et al. (2023).

4 Discussion

Both plots in Figure 4 show a remarkable agreement between the distribution of α-proton differential flow observed (red dashed curve) at $r = 1$ au with Wind and that predicted (solid blue curve) from collisional analysis for $r = 1$ au from PSP observations ($r = 0.1$ to 0.27 au). This may imply that the radial evolution of $\Delta v_{\alpha p}$ from the outer corona through to the inner heliosphere is governed by the effects of expansion and Coulomb collisions.

In general, collisional analysis was found to produce less dramatic changes in α-proton differential flow (this study) than in relative temperatures (Johnson et al., 2023). Utilizing Poisson statistics, the average uncertainty was calculated as $\sigma_{\Delta v_{\alpha p}} = 8.77$ %. The median predicted percent change in $\Delta v_{\alpha p}$ in going from PSP to Wind for the data set in this study was 23%, though the predicted change varied widely across the data set. The 25th- and 75th-percentile values of this percentage were 8% and 50%, indicating that the effect of collisions on $\Delta v_{\alpha p}$ was sometimes modest and other time more dramatic.

To date, this is the first study to directly apply the collisional analysis technique to ion differential flow. No preferential heating, acceleration or instabilities were included in the model (Eq. 8). Rather, it was assumed that the only collisions and expansion affect the relative drift between protons and α-particles. The strong agreement between the distributions of predicted and measured 1-au $\Delta v_{\alpha p}$-values suggests that the preferential acceleration of α-particles predominantly occurs closer to the Sun ($r \lesssim 0.1$ au), which is consistent with expectations for preferential heating (e.g., Kasper et al., 2017; Kasper and Klein, 2019).

Ideally, to test collisional analysis data should be taken simultaneously from two different spacecraft in the same steady solar wind stream. The differences in heliographic longitude between Wind and PSP are accounted for by populating the Wind data with measurements from a time period ranging from 10 days before to 10 days after each observation event, roughly the length of one Carrington rotation. Ensuring Wind has the largest possible number of kinetic states for a single solar wind stream and is statistically representative. Additionally, a solar wind stream is never fully steady and no accommodation has been made in this study for any intrinsic error propagating from spacecraft observations. These constraints and the limited coverage make it difficult to generalize about the full role of Coulomb collisions and expansion in the solar wind, thus any conclusion must include these caveats.

The continuation of the PSP mission will allow the data set to grow substantially, which will enable a more comprehensive study whose data set spans a larger number of solar-wind streams (i.e., a wider range of plasma conditions). Additionally, the perihelion of PSP's orbit is continuing to progress closer to the Sun, which may allow it to probe the region of the heliosphere where the preferential acceleration ions substantially occurs.

Data availability statement

The original contributions presented in the study are included in the article/supplementary material, further inquiries can be directed to the corresponding author.

Author contributions

EJ: Conceptualization, Formal Analysis, Investigation, Methodology, Software, Writing–original draft, Writing–review and editing. BAM: Funding acquisition, Resources, Supervision, Writing–review and editing. MMc: Data curation, Writing–review and editing. MS: Writing–review and editing. KGK: Writing–review and editing. PM: Writing–review and editing, Conceptualization.

Funding

The author(s) declare that no financial support was received for the research, authorship, and/or publication of this article. EJ and BAM are partially supported by the NSF Award No. 1931435. This research made use of PlasmaPy, a community-developed open-source Python package for plasma science PlasmaPy (2021).

Acknowledgments

We acknowledge the NASA Parker Solar Probe Mission and Solar Wind Electrons Alphas and Protons (SWEAP) team led by Professor Justin Kasper, NASA contract NNN06AA01C. Thanks to the Integrated Science Investigation of the Sun (IS⊙IS) Science Team (PI: David McComas, Princeton University) (McComas et al., 2014). The authors thank Brandy for assistance and fruitful discussions, this work is dedicated to her loving memory. The following software was utilized in this research: numpy (Harris et al., 2020), astropy (Astropy Collaboration et al., 2022), plasmapy (PlasmaPy, 2021), matplotlib (Hunter, 2007).

Conflict of interest

The authors declare that the research was conducted in the absence of any commercial or financial relationships that could be construed as a potential conflict of interest.

Publisher's note

References

Acuna, M. H., Ogilvie, K. W., Baker, D. N., Curtis, S. A., Fairfield, D. H., and Mish, W. H. (1995). The global geospace science program and its investigations. *Space Sci. Rev.* 71, 5–21. doi:10.1007/bf00751323

Alterman, B. L., Kasper, J. C., Stevens, M. L., and Koval, A. (2018). A comparison of alpha particle and proton beam differential flows in collisionally young solar wind. *Astrophysical J.* 864, 112. doi:10.3847/1538-4357/aad23f

Arfken, G. B., and Weber, H.-J. (2011). *Mathematical methods for physicists*. Germany: Elsevier.

Astropy Collaboration, Price-Whelan, A. M., Lim, P. L., Earl, N., Starkman, N., Bradley, L., et al. (2022). The astropy project: sustaining and growing a community-oriented open-source project and the latest major release (v5.0) of the core package. *ApJ* 935, 167. doi:10.3847/1538-4357/ac7c74

Durovcova, T., Nemecek, Z., and Safrankova, J. (2019). Evolution of the alpha-proton differential motion across stream interaction regions. *Astrophysical J.* 873, 24. doi:10.3847/1538-4357/ab01c8

Feldman, W. C., Asbridge, J. R., and Bame, S. J. (1974). The solar wind he2+ to h+ temperature ratio. *J. Geophys. Res.* 79, 2319–2323. doi:10.1029/JA079i016p02319

Fox, N. J., Velli, M. C., Bale, S. D., Decker, R., Driesman, A., Howard, R. A., et al. (2016). The solar probe plus mission: humanity's first visit to our star. *Space Sci. Rev.* 204, 7–48. doi:10.1007/s11214-015-0211-6

Griem, H. R. (1963). Validity of local thermal equilibrium in plasma spectroscopy. *Phys. Rev.* 131, 1170–1176. doi:10.1103/PhysRev.131.1170

Harris, C. R., Millman, K. J., van der Walt, S. J., Gommers, R., Virtanen, P., Cournapeau, D., et al. (2020). Array programming with NumPy. *Nature* 585, 357–362. doi:10.1038/s41586-020-2649-2

Hellinger, P., Matteini, L., Štverák, v., Trávníček, P. M., and Marsch, E. (2011). Heating and cooling of protons in the fast solar wind between 0.3 and 1 au: helios revisited. *J. Geophys. Res. Space Phys.* 116. doi:10.1029/2011JA016674

Hernández, R., Livi, S., and Marsch, E. (1987). On the he2+ to h+ temperature ratio in slow solar wind. *J. Geophys. Res. Space Phys.* 92, 7723–7727. doi:10.1029/JA092iA07p07723

Hernández, R., and Marsch, E. (1985). Collisional time scales for temperature and velocity exchange between drifting maxwellians. *J. Geophys. Res. Space Phys.* 90, 11062–11066. doi:10.1029/JA090iA11p11062

Hunter, J. D. (2007). Matplotlib: a 2d graphics environment. *Comput. Sci. Eng.* 9, 90–95. doi:10.1109/MCSE.2007.55

Johnson, E., Maruca, B. A., McManus, M., Klein, K. G., Lichko, E. R., Verniero, J., et al. (2023). Anterograde collisional analysis of solar wind ions. *Astrophysical J.* 950, 51. doi:10.3847/1538-4357/accc32

Kasper, J. C., Abiad, R., Austin, G., Balat-Pichelin, M., Bale, S. D., Belcher, J. W., et al. (2016). Solar wind electrons alphas and protons (sweap) investigation: design of the solar wind and coronal plasma instrument suite for solar probe plus. *Space Sci. Rev.* 204, 131–186. doi:10.1007/s11214-015-0206-3

Kasper, J. C., and Klein, K. G. (2019). Strong preferential ion heating is limited to within the solar alfvén surface. *Astrophysical J.* 877, L35. doi:10.3847/2041-8213/ab1de5

Kasper, J. C., Klein, K. G., Weber, T., Maksimovic, M., Zaslavsky, A., Bale, S. D., et al. (2017). A zone of preferential ion heating extends tens of solar radii from the sun. *Astrophysical J.* 849, 126. doi:10.3847/1538-4357/aa84b1

Kasper, J. C., Lazarus, A. J., and Gary, S. P. (2008). Hot solar-wind helium: direct evidence for local heating by alfvén-cyclotron dissipation. *Phys. Rev. Lett.* 101, 261103. doi:10.1103/PhysRevLett.101.261103

Kasper, J. C., Stevens, M. L., Korreck, K. E., Maruca, B. A., Kiefer, K. K., Schwadron, N. A., et al. (2012). Evolution of the relationships between helium abundance, minor ion charge state, and solar wind speed over the solar cycle. *Astrophysical J.* 745, 162. doi:10.1088/0004-637x/745/2/162

Larroche, O. (2021). An extended hydrodynamics model for inertial confinement fusion hohlraums. *Eur. Phys. J. D* 75, 297. doi:10.1140/epjd/s10053-021-00305-2

Livi, R., Larson, D. E., Kasper, J. C., Abiad, R., Case, A. W., Klein, K. G., et al. (2021). The solar probe analyzer -ions on parker solar probe. *Earth Space Sci. Open Archive* 20. doi:10.1002/essoar.10508651.1

Livi, R., Larson, D. E., and Rahmati, A. (2020). Psp solar wind electrons alphas and protons (sweap) span-a proton distribution function, partial moments, instrument frame. *level* 3 (l3), 7. doi:10.48322/ypyh-s325

Livi, S., Marsch, E., and Rosenbauer, H. (1986). Coulomb collisional domains in the solar wind. *J. Geophys. Res.* 91, 8045–8050. doi:10.1029/ja091ia07p08045

Marsch, E. (2006). Kinetic physics of the solar corona and solar wind. *Living Rev. Sol. Phys.* 3. doi:10.12942/lrsp-2006-1

Marsch, E., Mühlhäuser, K.-H., Rosenbauer, H., Schwenn, R., and Neubauer, F. M. (1982). Solar wind helium ions: observations of the helios solar probes between 0.3 and 1 au. *J. Geophys. Res. Space Phys.* 87, 35–51. doi:10.1029/JA087iA01p00035

Maruca, B. A., Bale, S. D., Sorriso-Valvo, L., Kasper, J. C., and Stevens, M. L. (2013). Collisional thermalization of hydrogen and helium in solar-wind plasma. *Phys. Rev. Lett.* 111, 241101. doi:10.1103/physrevlett.111.241101

Maruca, B. A., Kasper, J. C., and Bale, S. D. (2011). What are the relative roles of heating and cooling in generating solar wind temperature anisotropies? *Phys. Rev. Lett.* 107, 201101. doi:10.1103/PhysRevLett.107.201101

Maruca, B. A., Qudsi, R. A., Alterman, B. L., Walsh, B. M., Korreck, K. E., Verscharen, D., et al. (2023). *VizieR online data catalog: trans-heliospheric survey. Radial trends (Maruca+, 2023)*. USA: VizieR Online Data Catalog. J/A+A/675/A196.

McComas, D. J., Alexander, N., Angold, N., Bale, S., Beebe, C., Birdwell, B., et al. (2014). Integrated science investigation of the sun (isis): design of the energetic particle investigation. *Space Sci. Rev.* 204, 187–256. doi:10.1007/s11214-014-0059-1

McManus, M. D., Verniero, J., Bale, S. D., Bowen, T. A., Larson, D. E., Kasper, J. C., et al. (2022). Density and velocity fluctuations of alpha particles in magnetic switchbacks. *Astrophysical J.* 933, 43. doi:10.3847/1538-4357/ac6ba3

Mostafavi, P., Allen, R. C., McManus, M. D., Ho, G. C., Raouafi, N. E., Larson, D. E., et al. (2022). Alpha–proton differential flow of the young solar wind: parker solar probe observations. *Astrophysical J. Lett.* 926, L38. doi:10.3847/2041-8213/ac51e1

Neugebauer, M. (1976). The role of coulomb collisions in limiting differential flow and temperature differences in the solar wind. *J. Geophys. Res.* 81, 78–82. doi:10.1029/JA081i001p00078

Neugebauer, M. M., and Feldman, W. C. (1979). Relation between superheating and superacceleration of helium in the solar wind. *Sol. Phys.* 63, 201–205. doi:10.1007/bf00155710

Ogilvie, K. W., Chornay, D. J., Fritzenreiter, R. J., Hunsaker, F., Keller, J., Lobell, J., et al. (1995). Swe, a comprehensive plasma instrument for the wind spacecraft. *Space Sci. Rev.* 71, 55–77. doi:10.1007/bf00751326

PlasmaPy, C. (2021). *Plasmapy*. version 0.6.0 Zenodo.

Richardson, A. S. (2019). *NRL plasma formulary*. Washington, DC: Naval Research Laboratory.

Schmelz, J. T., Reames, D. V., von Steiger, R., and Basu, S. (2012). Composition of the solar corona, solar wind and solar energetic particles. *Astrophysical J.* 755, 33. doi:10.1088/0004-637x/755/1/33

Spitzer, L. (1962). *Physics of fully ionized gases*. China: Interscience Publishers.

Tracy, P. J., Kasper, J. C., Zurbuchen, T. H., Raines, J. M., Shearer, P., and Gilbert, J. (2015). Thermalization of heavy ions in the solar wind. *Astrophysical J.* 812, 170. doi:10.1088/0004-637x/812/2/170

Verscharen, D., Klein, K. G., and Maruca, B. A. (2019). The multi-scale nature of the solar wind. *Living Rev. Sol. Phys.* 16, 5. doi:10.1007/s41116-019-0021-0

Wilson, I., Lynn, B., Brosius, A. L., Gopalswamy, N., Nieves-Chinchilla, T., Szabo, A., et al. (2021). A quarter century of wind spacecraft discoveries. *Rev. Geophys.* 59, e2020RG000714. doi:10.1029/2020RG000714